THE JOURNAL OF PHYSICAL CHEMISTRY C

Article

pubs.acs.org/JPCC

Iron Phthalocyanine Electrodeposited Films: Characterization and Influence on Dopamine Oxidation

Cibely S. Martin,[†,‡] Carla Gouveia-Caridade,[‡] Frank N. Crespilho,[§] Carlos J. L. Constantino,[†] and Christopher M. A. Brett*[,‡]

[†]Departamento de Física, Faculdade de Ciências e Tecnologia, UNESP Universidade Estadual Paulista, Presidente Prudente, São Paulo, Brazil

[‡]Department of Chemistry, Faculty of Sciences and Technology, University of Coimbra, 3004-535 Coimbra, Portugal

[§]Instituto de Química de São Carlos, Universidade de São Paulo, São Carlos, São Paulo, Brazil

ABSTRACT: Electrodeposited films of iron phthalocyanine (FePc) were obtained by potential cycling and at fixed potential in 1,2-dichloroethane on glassy carbon and indium tin oxide electrodes and were characterized by cyclic voltammetry in aqueous solution. Films formed at constant potential were also characterized by electrochemical impedance spectroscopy. The mechanism of FePc film formation was investigated, with the FePc films being formed through interaction between the Pc macrocycle rings ($\pi-\pi$ aggregates). The electrochemical oxidation of dopamine (DA) at the FePc modified electrodes in aqueous solution was probed. Raman spectroscopy showed a specific interaction between Fe atoms of the FePc complex and $-NH_2$ groups in the dopamine molecules. The extensive interaction between the FePc film and DA in solution demonstrates the potential use of these modified electrodes for sensitive measurement of dopamine oxidation.

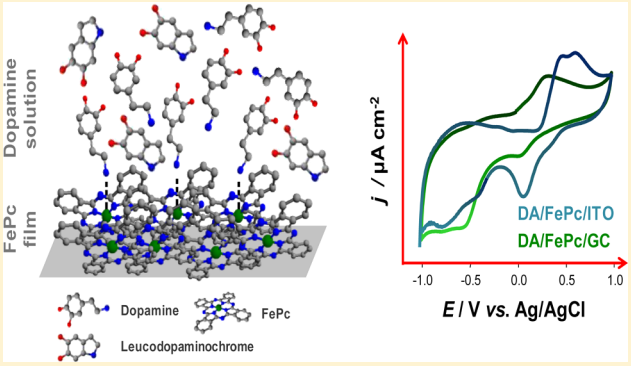

INTRODUCTION

Metallophthalocyanine complexes (MPc) are recognized for their chemical stability and excellent electrocatalytic activity, which are highly dependent on the central metal atom and on the substituent on peripheral sites of the phthalocyanine (Pc) macrocycle.[1−4] Different conducting substrates, such as glassy carbon, indium tin oxide (ITO), or gold, can be easily modified with MPc,[4−9] showing excellent electrochemical activity, with the MPc acting as electron mediator.

A large number of studies using MPc as electron mediators in electrochemical sensors have been reported, the mediation properties varying with the structure of the Pc macrocycle,[5,6] the metal center,[10,11] substrate,[5−7] or technique used for film formation.[5−13] MPc can also be used as substitutes for natural proteins, acting as the active center of an enzyme molecule with the same efficiency and selectivity.[14] Electrode modification with MPc has been carried out by different methods, such as Langmuir−Blodgett (LB),[12,15−17] electrostatic layer-by-layer (LbL),[4,18] physical vapor deposition (PVD),[12,19,20] casting,[21] and electrochemical deposition.[22,23] Recently, adsorption by click chemistry in carbon nanotube layers has been described.[8,13] Distinct behaviors of films on the same electrode substrate may be achieved through different deposition methods, enabling the development of chemical/electrochemical sensors with tunable properties.[12]

Among the different MPc complexes, iron phthalocyanine (FePc) has been widely used for electrode modification due to the possibility of interaction between the metallic iron center and nitrogen donors, here with the amino groups ($-NH_2$ groups) of various analyte molecules.[4,12,24,25] This interaction increases the sensitivity and selectivity of the modified electrodes for sensing molecules with $-NH_2$ groups, such as dopamine (DA), an important neurotransmitter.[4,8,25,26]

The aim of this work is to use voltammetric techniques and electrochemical impedance spectroscopy (EIS) to help in understanding what occurs during the preparation of FePc films on both glassy carbon (GC) and ITO-coated glass electrode surfaces in 1,2-dichloroethane. Following this, the electrochemical behavior of FePc films in the presence of DA in aqueous solution was examined. Evaluation of film formation and of an example electrode reaction is invaluable for evaluating these modified electrodes as electrochemical sensors.

EXPERIMENTAL SECTION

Reagents and Solutions. Electrodeposition was carried out using a 1.0 mmol L^{-1} iron phthalocyanine (FePc, Kodak, MM = 568.38 g mol^{-1}) solution prepared in 1,2-dichloroethane (DCE, Sigma-Aldrich) containing 0.1 mol L^{-1} tetrabutylam-

Special Issue: Kohei Uosaki Festschrift

Received: October 5, 2015
Revised: December 18, 2015
Published: January 29, 2016

DOI: 10.1021/acs.jpcc.5b09707
J. Phys. Chem. C 2016, 120, 15698−15706

monium perchlorate (TBAP, Fluka) as supporting electrolyte. The electrochemical characterization of the FePc films was performed in 0.1 mol L^{-1} potassium chloride (KCl, Fluka) aqueous solution. Dopamine oxidation was carried out in the presence of 1.0 mmol L^{-1} DA hydrochloride (Sigma) prepared in 0.1 mol L^{-1} KCl solution at pH 7.0. All aqueous solutions were prepared with Millipore Milli-Q nanopure water (resistivity ≥18 MΩ cm).

Instrumentation and Methods. The FePc films were formed on GC (0.28 cm^2) and ITO (ca.1.0 cm^2) electrode surfaces. All electrochemical experiments were performed in a conventional three-electrode cell, using the modified electrode as working electrode, an Ag/AgCl (sat. KCl) reference electrode, and a platinum wire as counter electrode. The voltammetric experiments were done using an Ivium CompactStat.e potentiostat (Ivium Technologies, Utrecht, Netherlands). Electrochemical impedance spectroscopy (EIS) experiments were carried out at open-circuit potential (OCP) using a Solartron 1250 Frequency Response Analyzer coupled to a Solartron 1286 Electrochemical Interface (Solartron Analytical, U.K.) controlled by Zplot Software. A sinusoidal voltage perturbation of amplitude 10 mV rms was applied in the frequency range from 65 kHz to 0.1 Hz with integration time of 60 s and 10 frequency steps per decade. Impedance spectra were analyzed by fitting to equivalent electrical circuits using ZView Software (Scribner Associates, USA).

UV−vis absorption spectroscopy, to monitor the growth of FePc films on the ITO electrode surface, was carried out using a Varian model Cary 50 spectrophotometer (Varian, USA) at 425 nm.

Characterization of modified ITO electrodes by micro-Raman spectroscopy was performed before and after electrochemical measurements in the absence and presence of DA. The Raman spectra were obtained with a Renishaw model in-Via spectrograph (Renishaw, U.K.) coupled to a Leica optical microscope, using a 785 nm laser line.

Formation of FePc Films by Electrodeposition. FePc films were electrodeposited by potential cycling and at constant potential on GC and ITO electrodes in solutions of 1 mmol L^{-1} FePc complex in 0.1 mol L^{-1} TBAP/DCE solution (under nitrogen atmosphere). Potential cycling was done between −1.8 and +1.5 V vs Ag/AgCl at 50 mV s^{-1}. Potentiostatic electrodeposition was performed at a constant applied potential of −1.5 V vs Ag/AgCl for 1800, 3600, and 7200 s. Potentials of −0.5 and +1.2 V vs Ag/AgCl were also applied during 3600 s to investigate the influence of electrodeposition potential.

Dopamine Oxidation at FePc Film Modified Electrodes. Evaluation of dopamine oxidation and the interaction of FePc film-modified electrodes with DA was done in aqueous solutions containing 1.0 mmol L^{-1} of DA in unbuffered 0.1 M KCl (pH ~7.0), in deoxygenated media, after N_2 bubbling during 20 min, cycling the potential from −1.0 to +1.0 V vs Ag/AgCl at 25 mV s^{-1}. Raman spectra were obtained before and after electrochemical characterization in the presence of DA to probe the chemical or physical interactions of FePc films with DA.

RESULTS AND DISCUSSION

Formation and Voltammetric Behavior of FePc Films on GC and ITO Electrodes by Potential Cycling. The electrodeposition of the FePc films on GC and ITO electrodes was carried out by potential cycling in a solution of 1 mmol L^{-1} FePc in 0.1 mol L^{-1} TBAP/DCE between −1.8 V and +1.5 V vs Ag/AgCl at 50 mV s^{-1} during 30 potential cycles, the modified electrodes then being characterized by cyclic voltammetry in 0.1 mol L^{-1} KCl aqueous solution at 25 mV s^{-1}.

The increase in peak currents with increasing number of cycles was observed for both electrode materials, as shown in Figure 1, due to the growth of the FePc film on the electrode

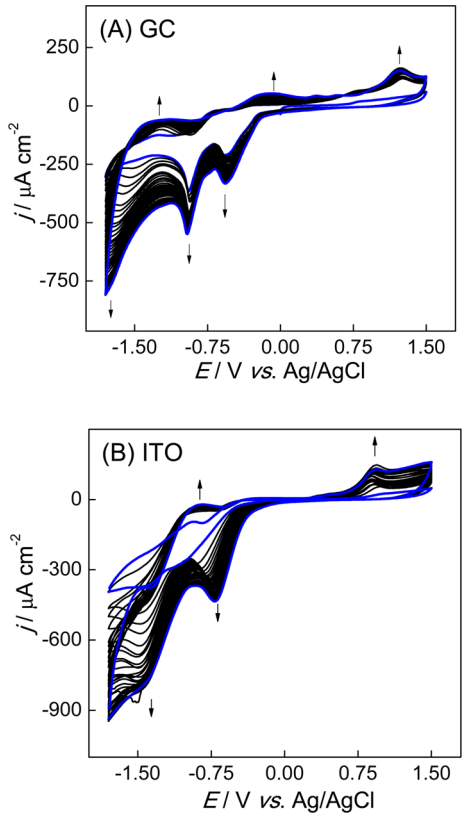

Figure 1. Cyclic voltammetric response for the electrodeposition of 1.0 mmol L^{-1} FePc in 0.1 mol L^{-1} TBAP/DCE on (A) GC and (B) ITO electrodes, applying 30 potential cycles between −1.8 and +1.5 V vs Ag/AgCl at 50 mV s^{-1}.

surface; however, differences in the voltammetric profiles for GC and ITO electrode substrates were seen, which suggests that different interactions between the film and the electrode surface occur.

The first redox process observed in the positive scan in the negative potential region at around −1.3 V for FePC/GC and −1.0 V vs Ag/AgCl for FePc/ITO electrodes is attributed to ring oxidation $[Fe^{I}Pc^{3-}]^{-2} \rightarrow [Fe^{I}Pc^{2-}]^{-1} + e^{-}$, with corresponding reverse cathodic peaks at ~ −1.50 V in the first cycles.[27−31] A second redox process, anodic peak potential −0.13 V (cathodic peak potential −0.56 V), was observed at the FePc/GC electrode and is due to the metal center $[Fe^{I}Pc^{2-}]^{-1} \rightarrow [Fe^{II}Pc^{2-}] + e^{-}$.[27−31] At the FePC/ITO electrode, this was observed in the first potential cycle at a more negative potential than at the FePc/GC electrode, with the anodic peak at −0.43 V and the cathodic peak at −1.07 V, then becoming superimposed with the $[Fe^{I}Pc^{3-}]^{-2}/[Fe^{I}Pc^{2-}]^{-1}$ redox couple; such superposition was also observed for FePc films evaluated in aqueous solution (discussed below). The irreversible anodic processes at +0.82 and +0.92 V vs Ag/AgCl, for GC and ITO electrodes, respectively, in small peaks in the first cycle are related to monomer cation radical formation, and from the second cycle onward much larger peaks appear

DOI: 10.1021/acs.jpcc.5b09707
J. Phys. Chem. C 2016, 120, 15698−15706

Table 1. Attribution of Peak Potentials in the FePc Potential Cycling Electrodeposition Process on GC and ITO Electrodes in the 30th Potential Cycle; solution of 1.0 mmol L^{-1} FePc in 0.1 mol L^{-1} TBAP/DCE[a]

	$[Fe^{I}Pc^{3-}]^{-2}/[Fe^{I}Pc^{2-}]^{-1}$		$[Fe^{I}Pc^{2-}]^{-1}/[Fe^{II}Pc^{2-}]$		$[Fe^{II}Pc^{2-}]/[Fe^{II}Pc^{1-}]^{+1}$
electrode	E_{pa}/V	E_{pc}/V	E_{pa}/V	E_{pc}/V	E_{pa}/V
GC	−1.31	−1.70	−0.13	−0.56	+1.20
ITO	−0.87	−1.50	−0.43[b]	−0.70[b]	+0.92

[a]Potential values vs Ag/AgCl. [b]First potential cycle during electrodeposition.

attributed to an irreversible second phthalocyanine ring oxidation in the FePc film: $[Fe^{II}Pc^{2-}] \rightarrow [Fe^{II}Pc^{1-}]^{+1} + e^{-}$ at +1.20 V (GC) and at 0.90 V vs Ag/AgCl (ITO). According to the literature,[30−34] the cation radical formed by oxidation of the pyrrole groups at high positive potential attacks a neutral FePc molecule present in solution and leads to the commencement of film formation. Ring oxidation $[Fe^{II}Pc^{2-}] \rightarrow [Fe^{II}Pc^{1-}]^{+1} + e^{-}$ is observed only after the first potential cycle, an increase in peak current occurring with the increase in the number of cycles, indicating that this oxidation occurs only on the film formed at the electrode surface.

The cathodic peaks at ∼−0.80 V for both electrode materials, the baseline-subtracted peak current being independent of scan number, are seen in the absence of FePc and can be ascribed to interactions between the electrode substrate and the 1,2-dichloroethane solvent.

The values of peak potentials after the 30 cycles and the respective attributions are summarized in Table 1.

Cyclic Voltammetry Characterization in Aqueous Solution. In 0.1 mol L^{-1} KCl (Figure 2), the GC and ITO electrodes modified with FePc films showed one redox process at E_m −0.85 V and −0.76 V vs Ag/AgCl ($E_m = (E_{pa} + E_{pc})/2$), respectively, ascribed to the redox couple $[Fe^{I}Pc^{3-}]^{-2}/[Fe^{I}Pc^{2-}]^{-1}$ (Figure 2A).[27−31] Similar potentials have been observed with films formed from analogous iron phthalocyanine complexes in the literature,[30,32−34] confirming that this redox process is related to the phthalocyanine ring.

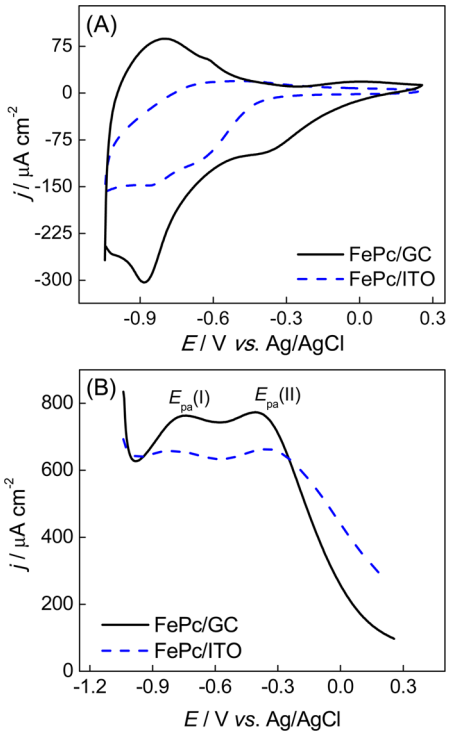

Figure 2. Response of the FePc/GC and FePc/ITO electrodes in 0.1 mol L^{-1} KCl aqueous solution obtained by (A) cyclic voltammetry at 25 mV s^{-1} and (B) differential pulse voltammetry at 10 mV s^{-1} and pulse amplitude of 50 mV vs Ag/AgCl.

The cathodic peaks at −0.64 V for the FePc/ITO and at −0.38 V vs Ag/AgCl for the FePc/GC electrode can be attributed to oxygen reduction because FePc complexes have electrocatalytic activity toward oxygen reduction.[33,35,36] The interaction between FePc complexes and molecular oxygen occurs through charge transfer from the electron metal center to the O_2 π^* orbitals, leading to weakening of the O−O bond, in this way allowing O_2 reduction to occur more easily.[35] With a continuous flow of nitrogen gas to remove dissolved oxygen, a large decrease in the oxygen reduction peak was observed as well as a separation of the peaks attributed to the FePc film redox process. The separation of peak potentials was better seen by differential pulse voltammetry (Figure 2B). Thus, the anodic peaks at −0.74 and −0.78 V vs Ag/AgCl can be ascribed to the macrocycle oxidation ($[Fe^{I}Pc^{3-}]^{-2} \rightarrow [Fe^{I}Pc^{2-}]^{-1}$) and those at −0.40 V and −0.34 V vs Ag/AgCl can be ascribed to the redox couple $[Fe^{I}Pc^{2-}]^{-1} \rightarrow [Fe^{II}Pc^{2-}]$, for the FePc/GC and FePc/ITO modified electrodes, respectively.

Constant Potential Electrodeposition of FePc Films on GC Electrodes. The influence of different electrodeposition parameters for constant applied potential electrodeposition was evaluated for FePc film growth using the GC electrode as substrate. FePc films were obtained by applying a potential of −1.5, −0.5, or +1.2 V vs Ag/AgCl in 0.1 mol L^{-1} TBAP/DCE for 3600 s. The FePc films were characterized by cyclic voltammetry and EIS in 0.1 mol L^{-1} KCl aqueous solution. For both characterization methods, only the FePc film obtained at −1.5 V vs Ag/AgCl showed electrochemical behavior characteristic of these types of film, while for those obtained at the other potentials the behavior is mainly that of the bare GC electrode ; that is, very little FePc film was deposited. The corresponding cyclic voltammograms for FePc films formed at different constant applied potentials (Figure 3), showed two redox processes at E_m (I) −0.95 V and E_m (II) −0.70 V vs Ag/AgCl due to $[Fe^{I}Pc^{3-}]^{-2}/[Fe^{I}Pc^{2-}]^{-1}$ and $[Fe^{I}Pc^{2-}]^{-1}/Fe^{II}Pc^{2-}]$, respectively. Oxygen reduction was also observed for unmodified and modified GC electrode (see Figure 3B).

As observed in electrodeposition by potential cycling (see Figure 1) the peak potential at +1.2 V vs Ag/AgCl is unlikely to be related to film formation via the attack on neutral molecules present in solution of the radicals formed, as proposed in the literature,[30−34] because ring oxidation is observed only in the second cycle. For film formation at constant applied potential, films with characteristic FePc behavior were only obtained at −1.5 V vs Ag/AgCl, which confirms the prior necessity of FePc reduction for film formation. The negative applied potential allows the reduction of the metallic center to Fe(I) and formation of $[Fe^{I}Pc^{3-}]^{-2}$ species, favoring the formation of a more negative charge on the Pc macrocycle, increasing the $\pi-\pi$

DOI: 10.1021/acs.jpcc.5b09707
J. Phys. Chem. C 2016, 120, 15698−15706

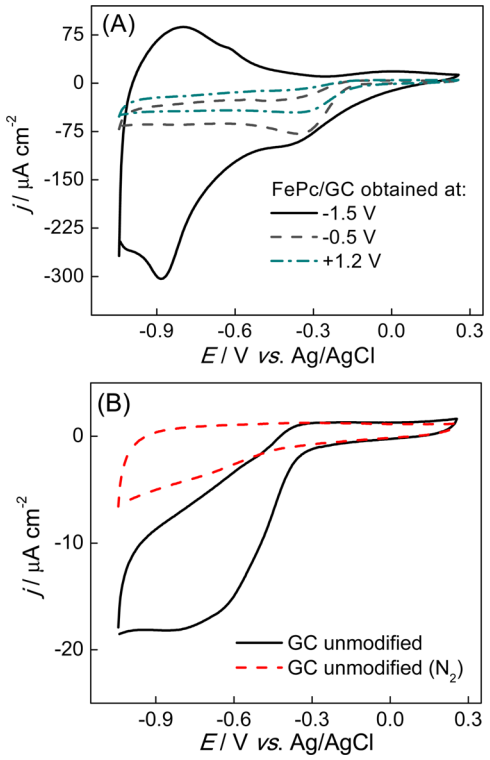

Figure 3. Cyclic voltammograms obtained with (A) GC electrode modified with FePc films formed at −1.5, −0.5, and +1.2 V vs Ag/AgCl. (B) Unmodified GC electrode (d) with and (e) without a continuous flow of nitrogen gas. Supporting electrolyte: 0.1 mol L^{-1} KCl; scan rate 25 mV s^{-1}.

interaction between the Pc macrocycle rings (formation of $\pi-\pi$ aggregates). This suggests that the formation of reduced species ($[Fe^{I}Pc^{3-}]^{-2}$) can be the rate-determining step for FePc film formation.

Impedance spectra obtained at open-circuit potential (OCP) (Figure 4) give information on the electrical properties of the FePc films and provide complementary information to cyclic voltammetry. As expected from cyclic voltammetry, only the GC electrode modified at −1.5 V vs Ag/AgCl showed behavior very different from that of the unmodified GC electrode, also reflected in the values of OCP, which were ∼0.10 V for modification at −0.5 and 1.2 V vs Ag/AgCl and 0.02 V for films formed at −1.50 V vs Ag/AgCl (0.28 V for bare GCE). A semicircle in the high-frequency range (charge transfer control) and a linear part at lower frequency range (diffusion control) was observed for the GC electrode modified at −1.5 V vs Ag/AgCl. For GC electrodes modified at −0.5 V and +1.2 V vs Ag/AgCl no films were formed, and thus the difference observed in the low-frequency region (difference in impedance phase angle) can be ascribed to solvent adsorption during electrodeposition.

Impedance spectra were also obtained using GC electrode modified with FePc films at −1.5 V vs Ag/AgCl for 1800, 3600, and 7200 s, as shown in Figure 4B.

Fitting to equivalent electrical circuits was done with the typical Randles-type circuit shown in Figure 4C. It comprises a cell resistance, R_{Ω}, in series with a parallel combination of a constant phase element, CPE, and a charge transfer resistance, R_{ct}, together with a Warburg impedance, Z_w. The CPE was modeled as a nonideal capacitor, given by CPE = $-1/(Ci\omega)^{\alpha}$, where C is the capacitance, which describes the charge separation at the double-layer interface, ω is the frequency in rad s^{-1}, and the α exponent is due to the nonuniformity and heterogeneity of the surface ($0.5 < \alpha < 1$). The Warburg impedance was modeled as an open-circuit finite Warburg element, according to $Z_w = R_{dif}\coth[(\tau i\omega)^{\alpha}]/(\tau i\omega)^{\alpha}$, where R_{dif} is the diffusion resistance of electroactive species, τ is a time constant ($\tau = l^2/D$, where l is the effective diffusion thickness, and D is the effective diffusion coefficient of the species), and $\alpha < 0.5$. The values of the equivalent circuit elements obtained from the fittings are summarized in Table 2. The errors in the fitting of the experimental values to the equivalent circuit were ∼1% for the R_{Ω}, α, and α_{wo} and ∼6% for the other parameters (capacitance, R_{wo} and R_{ct}).

An increase in the diameter of the semicircle with increase in electrodeposition time can be due to the increase in film thickness, as previously noted.[37,38] At the FePc/GC with FePc film formed during 1800 s, no semicircle was observed, suggesting that diffusion control is predominant over the whole frequency range, a behavior commonly observed with ultrathin films.[37] An increase in the capacitance and R_{ct} values and a decrease in α with increasing electrodeposition time are found. This suggests that the growth of the FePc film occurs by interaction between Pc macrocyclic rings and formation of $\pi-\pi$ aggregates,[26] with the increase in the number of FePc aggregates decreasing the homogeneity of the surface and in this case an increase in the charge-transfer resistance. Thus, the FePc film that formed at −1.5 V vs Ag/AgCl for 3600 s was used for further studies.

The FePc films showed good stability and reproducibility in aqueous solution; that is, increasing the number of potential cycling scans, the time of immersion in aqueous solution, and the storage time at room temperature had no influence on the electrochemical behavior of the modified electrodes, which can be ascribed to strong $\pi-\pi$ aggregations stabilizing the film structure.

Dopamine Oxidation and FePc Film Interaction with Dopamine in Solution. Figure 5 shows cyclic voltammograms obtained for the unmodified GC and GC electrode modified with FePc film in the presence of 1.0 mmol L^{-1} DA in 0.1 mol L^{-1} KCl solution at pH 7.0. The unmodified GC electrode shows a reversible pair of peaks with E_m = 0.009 V vs Ag/AgCl due to the hydroquinone/quinone redox couple (dopamine oxidation to dopamine *ortho*-quinone (DOQ)),[39] with the irreversible peak at 0.51 V vs Ag/AgCl being due to the oxidation of leucodopaminochrome to dopaminochrome, related to dopamine cyclization.[39] The cathodic peak at ∼−0.8 V can be ascribed to reduction of surface oxides and of any remaining dissolved oxygen, the amount of which is minimized by a continuous flow of nitrogen gas.

DA can also undergo spontaneous electrochemical polymerization, forming films on various surfaces,[40,41] or cyclization in neutral or basic aqueous solution.[39] The possible electrochemical and cyclization reactions of the DA molecule in aqueous solution are illustrated in Scheme 1.

In comparison, the FePc film-modified GC electrode in the presence of DA showed only the reversible redox process related to the hydroquinone/quinone redox couple at E_m = 0.14 V vs Ag/AgCl. The decrease in the both anodic and cathodic peak currents was ascribed to $[Fe^{I}Pc^{3-}]^{-2}/[Fe^{I}Pc^{2-}]^{-1}$ and $[Fe^{I}Pc^{2-}]^{-1}/[Fe^{II}Pc^{2-}]$ redox processes, and that of the oxidation peak current of the leucodopaminochrome/dopaminochrome process can be attributed to the interactions between the Fe atoms and $-NH_2$ group of DA molecule (Scheme 2). Thus, the FePc/$-NH_2$ interaction decreases the number of

DOI: 10.1021/acs.jpcc.5b09707
J. Phys. Chem. C 2016, 120, 15698−15706

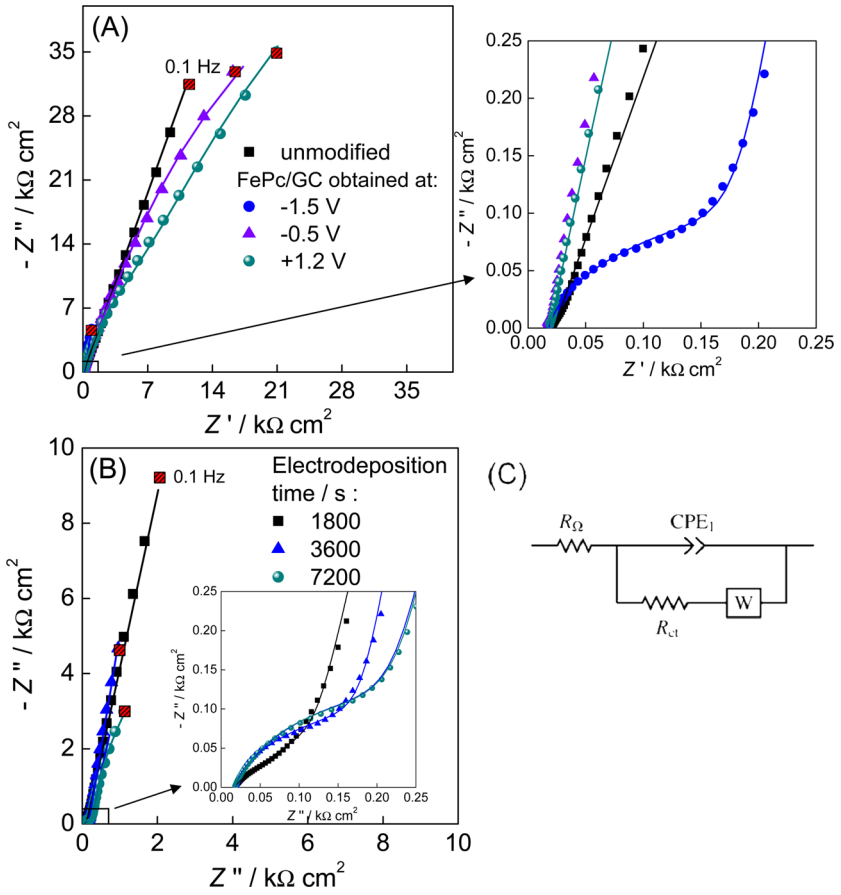

Figure 4. Complex plane impedance spectra of GC electrodes modified with FePc films in 0.1 mol L^{-1} KCl solution at OCP. Magnifications of the high-frequency part are also shown. Lines indicate equivalent circuit fitting. Films formed by electrodeposition in 1.0 mmol L^{-1} FePc in 0.1 mol L^{-1} TBAP/DCE: (A) At different potentials (−1.5, −0.5, and +1.2 V vs Ag/AgCl) for 3600 s. (B) For different times (1800, 3600, and 7200 s) at −1.5 V vs Ag/AgCl. (C) Equivalent electrical circuit used to fit the impedance spectra.

Table 2. Parameters Obtained from Impedance Spectra of the GC Electrode Modified with FePc Films Formed at −1.5 V vs Ag/AgCl for Different Times[a]

electrodeposition time/s	R_Ω/Ω cm^2	R_{ct}/Ω cm^2	CPE/μF cm^{-2} s$^{\alpha-1}$	α	R_{diff} (W_0)/Ω cm^2	τ/s	α_{Wo}
1800	14.8				302	0.030	0.43
3600	17.8	107	41.2	0.84	260	0.055	0.45
7200	17.3	192	99.7	0.76	237	0.068	0.44

[a]Parameters obtained by fitting to the equivalent circuits of Figure 5C; frequency range 65 kHz to 0.1 Hz.

active metallic centers as well as the cyclization reaction of DA molecules in solution. Furthermore, after measurements in DA solution, a cyclic voltammogram was recorded in blank electrolyte solution (0.1 mol L^{-1} KCl) in the absence of DA, and the peaks associated with the hydroquinone/quinone redox couple were also observed (Figure 5, curve 3). This suggests strong adsorption of DA molecules on the FePc film surface, which preserves their redox activity. The DA adsorption on the FePc film surface was confirmed by the linear dependence of peak current with scan rate (data not shown). The peaks due to the hydroquinone/quinone redox couple in 0.1 mol L^{-1} KCl solution decrease with time due to desorption of DA.

In the literature, several reports[4,8,26,41] describe the possible interaction between FePc and $-NH_2$ groups in different molecules. Coates and Nyokong[8] related the formation of FePc films by click chemistry between carbon nanotubes and 4-ethylpyridine moieties to strong axial bonds of FePc complexes and pyridine. Zucolotto et al.[4] found that layer-by-layer films constituted by PAH (poly(allylamine hydrochloride)) and FeTsPc (iron tetrasulfonated phthalocyanine) are formed by the interaction between the Fe atoms and unprotonated $-NH_2$ groups from PAH; the fact that the electroactivity of DA could not be detected due to the screening effect of PAH on the FeTsPc films suggested that for DA determination the metal center should be available to axial interactions. On the basis of the results reported here and those in the literature[4,8,26,41] the FePc films show excellent potential for the electroanalysis of DA. The increase in the sensitivity and selectivity of the sensor should be possible through protonation of the $-NH_2$ groups, that is, through control of the pH of the solution.[4,8,39]

A similar behavior was observed for ITO electrodes modified with FePc films during different electrodeposition times, with the increasing thicknesses being observed by monitoring the growth of the FePc film by UV−vis absorption spectroscopy (Figure 6). The absorbance at 425 nm ascribed to the B band[4]

DOI: 10.1021/acs.jpcc.5b09707
J. Phys. Chem. C 2016, 120, 15698−15706

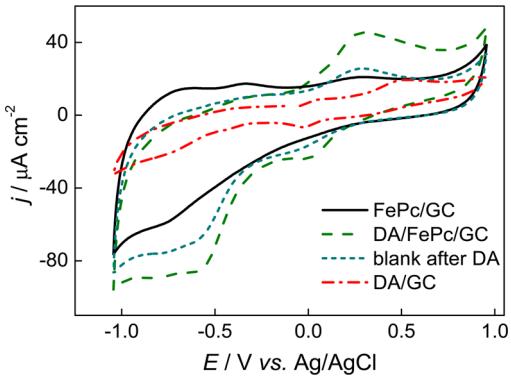

Figure 5. Cyclic voltammetric responses, recorded at 25 mV s^{-1} in 0.1 mol L^{-1} KCl solution pH ~ 7.0, for the FePc/GC electrode in the absence and presence of 1 mmol L^{-1} of DA and in blank solution after measurement of DA. For comparison: CV obtained with unmodified GC electrode in the presence of 1 mmol L^{-1} of DA. Measurements were carried out under a continuous flow of nitrogen gas.

Scheme 1. Mechanism of the Electrochemical and Cyclization Reaction of DA

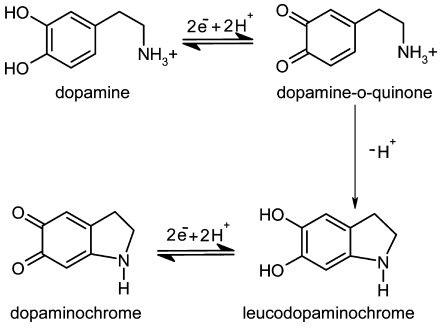

increased linearly with electrodeposition time, indicating linear growth.

At modified ITO electrodes, some decrease in the anodic peak corresponding to the cyclic dopamine species (leucodopaminochrome) and an increase in the hydroquinone/*o*-quinone process with increasing FePc film thickness can be seen in Figure 7. This can be attributed to an increase in the number of the metal centers available for interactions with $-NH_2$ from the DA molecule that diffuse to within the films. DA cyclization is minimized on the electrode surface and the reversible process of hydroquinone/quinone becomes favored, as indicated before.

Electrochemical measurements showed a strong interaction of DA molecules with electrodeposited FePc films, independent of the electrode material. This interaction is sufficiently strong to minimize the DA cyclization reaction and increase the proportion of electroxidation of DA in aqueous solution. Additionally, the peak current of the hydroquinone/quinone redox couple obtained with the modified electrode was higher than that at the unmodified electrode, suggesting that FePc/GC electrodes can serve as catalysts for DA oxidation and consequent quantification in aqueous solution.

To compare possible changes in the molecular structure of FePc or supramolecular arrangement of the FePc film, before and after electrochemical measurements in the presence of 1.0 mmol L^{-1} DA, we recorded Raman spectra of ITO modified with FePc films as well as of FePc powder, as shown in Figure 8A. All spectra showed the same number of Raman bands, and

Scheme 2. Schematic Representation of Interaction between the Fe Atom of the FePc Film Surface and $-NH_2$ Groups from DA Molecules[a]

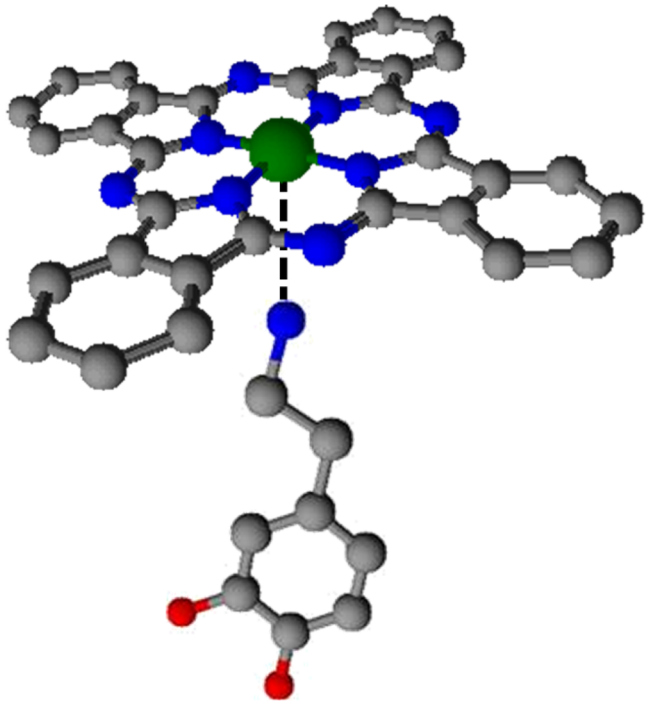

[a]Representation of colors: green (Ni), grey (C), red (O), and blue (N); the H atoms are not shown.

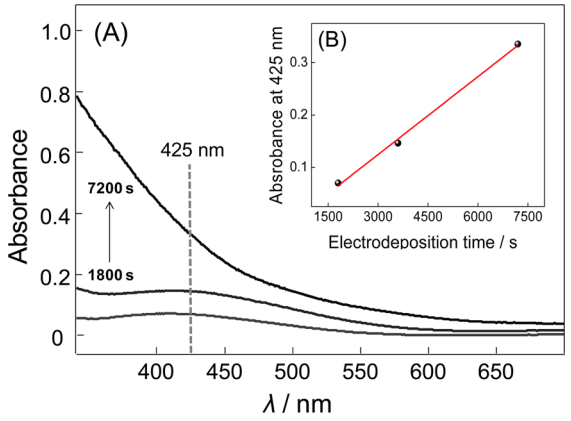

Figure 6. (A) UV−vis absorption spectra for FePc films electrodeposited on ITO electrodes for 1800, 3600, and 7200 s at −1.5 V vs Ag/AgCl. (B) Dependence of the absorbance at 425 nm as a function of electrodeposition time.

most of the frequency changes were <4 cm^{-1}. The band ascribed to C═C and C═N of pyrrole stretching is the exception, as shown in Figure 8B. Table 3 summarizes the assignments of the Raman bands.[4,19,20,26,28,42] Simic-Glavaski et al.[42] described the changes in C═C vibration modes to oxidation of the pyrrole ring and delocalized charge within the ring. Spiro and Strekas[43] proposed that electron transfer from the iron center to π orbitals of the Pc macrocycle may cause a frequency shift in the Raman spectra. On the basis of these results, the electrodeposition process at negative potential (−1.5 V vs Ag/AgCl) and consequent formation of Fe(I) species can allow electron transfer from the iron center to π

DOI: 10.1021/acs.jpcc.5b09707
J. Phys. Chem. C 2016, 120, 15698−15706

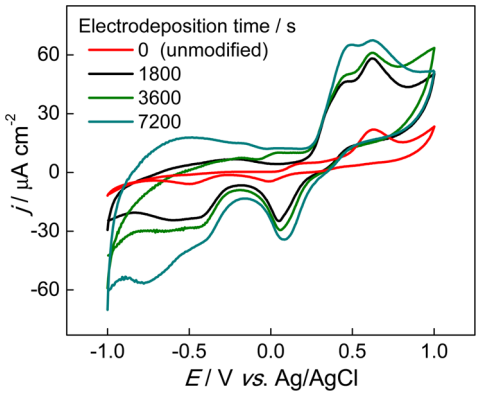

Figure 7. Cyclic voltammetric response in 1.0 mmol L^{-1} DA + 0.1 mol L^{-1} KCl solution of the ITO electrode unmodified and modified with FePc film obtained for different electrodeposition times: 1800, 3600, and 7200 s at −1.5 V vs Ag/AgCl. Measurements were carried out under a continuous flow of nitrogen gas.

orbitals of the pyrrole rings, which causes a shift of the band at 1512 (powder) to 1519 cm^{-1} (film).

For the FePc film after measurements in DA solution, a shift to lower frequency from 1519 to 1515 cm^{-1} occurred that can be ascribed to the interaction of $-NH_2$ groups from DA molecules with Fe atoms in the FePc film.[4,26] The DA/FePc interaction may minimize the electronic deficiency of the metal center that leads to a decrease in the vibration frequency of the Pc macrocycle, with the band being similar to that obtained with the powder.

Another important change in the spectra was the relative intensity of the band ascribed to the Pc macrocycle vibration (I_{R1}) and C−H out-of-plane bending (I_{R2}), as shown in detail in Figure 8C. The ratio I_{R1}/I_{R2} (in-plane/out-of-plane) for the FePc powder was 0.52, while for the FePc film it was 0.93, indicating a possible molecular organization of the FePc film on the ITO surface; in addition, the bandwidth decreases from the FePc powder to the FePc film, which is consistent with the hypothesis of film organization. A similar change was observed by Simic-Glavaski and coworkers[42] for iron tetrasulfonated phthalocyanine FeTsPc, where the increase in the relative intensity ratio between and in-plane/out-of-plane supports a model in which FeTsPc molecules have an edge-on orientation to the electrode surface.

A decrease in the I_{R1}/I_{R2} ratio from 0.92 to 0.69 and an increase in bandwidth were both observed in the Raman spectra of FePc films after measurements in DA-containing solution,

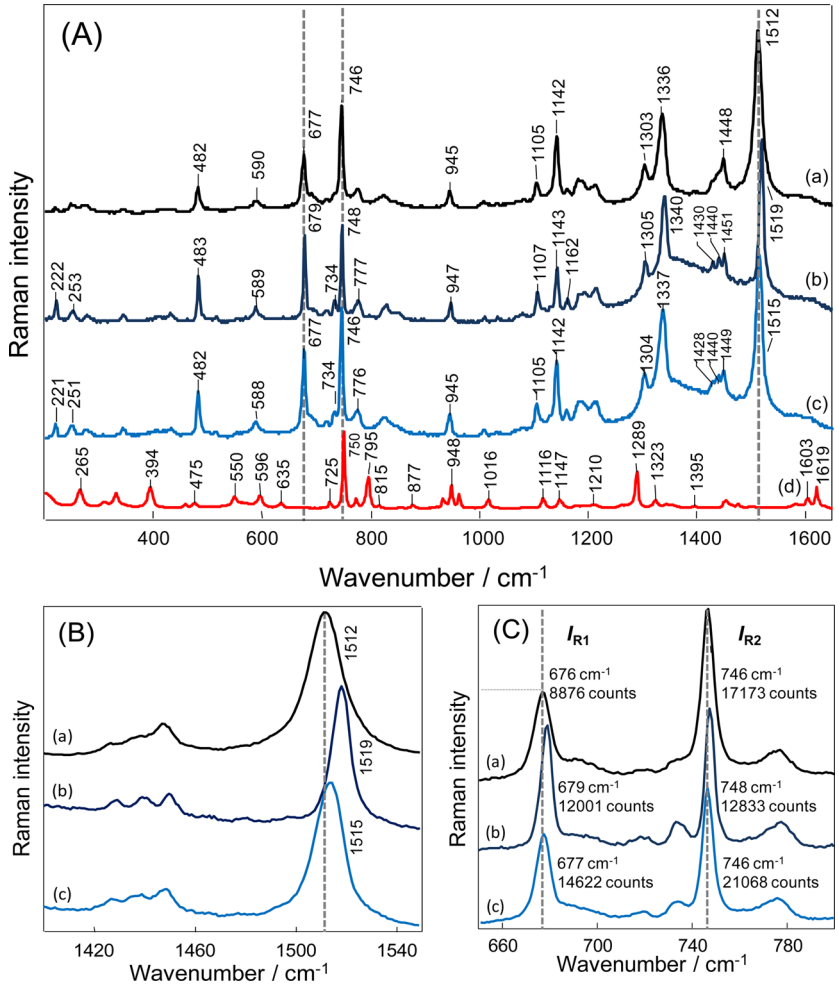

Figure 8. (A) Raman spectra, using the 785 nm laser line, for (a) FePc complex (powder); FePc film on ITO electrode surface (b) before and (c) after electrochemical measurements in 1 mmol L^{-1} DA solution; and (d) DA powder. (B) Magnification of wavenumber range 1400−1550 cm^{-1}, showing the difference of relative intensity of the band ascribed to in-plane macrocycle vibration (I_{R1}) and C−H bending out-of-plane (I_{R2}). (C) Magnification of wavenumber range 650−800 cm^{-1}, showing the shift of the band ascribed to C═C and C═N pyrrole stretching.

DOI: 10.1021/acs.jpcc.5b09707
J. Phys. Chem. C 2016, 120, 15698−15706

Table 3. Peak Assignment for the Raman Data for FePc Film Powder and FePc Film on ITO Electrode before and after Electrochemical Measurements in 1.0 mmol L^{-1} DA Solution

FePc (powder)	FePc (film)		assignments
	before	after	
	222	221	N−Fe
	253	251	N−Fe
482	483	483	isoindole deformation
677	679	677	Macrocycle vibration, C−N−C, N−Fe stretching, pyrrole expanding, benzene deformation
746	748	749	C−H out-of-plane bending
776	777	776	isoindole N−Fe stretching
824	829	824	pyrrole N−Fe stretching, benzene expanding, C−N−C in-plane bending
945	947	946	N−Fe C−N−C in-plane bending, isoindole deformation
1105	1105	1105	C−H in-plane bending, isoindole N−Fe stretching
1142	1142	1142	C−H in-plane bending
1303	1305	1304	isoindole N−Fe stretching, C−H in-plane bending
1336	1340	1347	pyrrole stretching, isoindole N−Fe stretching, C−H C−N−C in-plane bending
1448	1451	1449	isoindole stretching, ring stretching, pyrrole N−Fe C−H in-plane bending
1512	1519	1515	C═C, C═N pyrrole stretching, C−N−C stretching, pyrrole expanding, C−H in-plane bending

which could be due to DA/FePc interactions. The presence of DA in the FePc film can cause a subtle charge delocalization that affects the electronic film organization.

Voltammetric and Raman characterization showed extensive interaction between the FePc film and DA in solution. At low micromolar concentrations of dopamine, the deadsorption of DA molecules from the FePc film can be expected to not be important for the use of these modified electrodes for sensitive electrochemical sensing of dopamine, an aspect to be exploited in future work.

CONCLUSIONS

Electroactive films of iron phthalocyanine were obtained by electrodeposition in potentiodynamic and potentiostatic modes. Electrochemical impedance spectra and cyclic voltammograms in aqueous solution of GC electrode modified with FePc films obtained by electrodeposition at constant potential showed that the reduction of the metal center at −1.5 V vs Ag/AgCl is the rate-determining step for FePc film growth. The growth of FePc film on electrode surface occurs by the interaction between Pc macrocycles, forming $\pi-\pi$ aggregates. These aggregates formed have a direct influence on the homogeneity of the surface and on the charge-transfer process. The electroactivity of FePc films for DA oxidation proceeds through FePc/$-NH_2$ interactions. Thus, FePc films can be used to enhance electron transfer between the electrode and DA, and thence sensitivity, because dopamine cyclization is minimized and the hydroquinone/quinone process is favored.

AUTHOR INFORMATION

Corresponding Author

*Tel: +351 239854470. Fax: +351 239827703. E-mail: cbrett@ci.uc.pt.

Notes

The authors declare no competing financial interest.

ACKNOWLEDGMENTS

Financial support from Fundação para a Ciência e a Tecnologia (FCT), Portugal PTDC/QUI-QUI/116091/2009, POPH, POCH, POFC-QREN (cofinanced by FSE and European community FEDER funds through the program COMPETE - Programa Operacional Factores de Competitividade under the projects PEst-C/EME/UI0285/2013 and CENTRO-07-0224-FEDER-002001 (MT4MOBI)) is gratefully acknowledged. C.S.M thanks FAPESP for doctoral fellowships 2012/25140-7 and 2013/22087-0. C.G.-C. thanks FCT for postdoctoral fellowship SFRH/BPD/46635/2008.

REFERENCES

(1) Costamagna, J.; Ferraudi, G.; Matsuhiro, B.; Campos-Vallette, M.; Canales, J.; Villagrán, M.; Vargas, J.; Aguirre, M. J. Complexes of macrocycles with pedant arms as models for biological molecules. *Coord. Chem. Rev.* **2000**, *196*, 125−164.

(2) Mashazi, P. N.; Nombona, N.; Muchindu, M.; Vilakazi, S. Metallophthalocyanines and metalloporphyrins as electrocatalyst: a case of hydrogen peroxide and glucose detection. *J. Porphyrins Phthalocyanines* **2012**, *16*, 741−753.

(3) Claessens, C. G.; Blau, W. J.; Cook, M.; Hanack, M.; Nolte, R. J. M.; Torres, T.; Wohrle, D. Phthalocyanines and phthalocyanines analogues: the quest for applicable optical properties. *Monatsh. Chem.* **2001**, *132*, 3−11.

(4) Zucolotto, V.; Ferreira, M.; Cordeiro, M. R.; Constantino, C. J. L.; Balogh, D. T.; Zanatta, A. R.; Moreira, W. C.; Oliveira, O. N. Unsual interactions binding iron tetrasulfonated phthalocyanine and poly(allylamine hydrochloride) in layer-by-layer films. *J. Phys. Chem. B* **2003**, *107*, 3733−3737.

(5) Zagal, J. H.; Griveau, S.; Silva, J. F.; Nyokong, T.; Bedioui, F. Metallophthalocyanine-based molecular materials as catalysts for electrochemical reactions. *Coord. Chem. Rev.* **2010**, *254*, 2755−2791.

(6) Valli, L. Phthalocyanine-based Langmuir-Blodgett films as chemical sensor. *Adv. Colloid Interface Sci.* **2005**, *116*, 13−44.

(7) Apetrei, C.; Medina-Plaza, C.; de Saja, J. A.; Rodriguez-Mendez, M. L. Electrochemical characterization of dilithium phthalocyanine carbonaceous electrodes. *J. Porphyrins Phthalocyanines* **2013**, *17*, 522−528.

(8) Coates, M.; Nyokong, T. Characterization of glassy carbon electrodes modified with carbon nanotubes and iron phthalocyanine through grafting and click chemistry. *Electrochim. Acta* **2013**, *91*, 158−165.

(9) Bedioui, F.; Griveau, S.; Nyokong, T.; Appleby, A. J.; Caro, C. A.; Gulppi, M.; Ochoa, G.; Zagal, J. H. Tuning the redox properties of metalloporphyrin- and metallophthalocyanine-based molecular electrodes for the highest electrocatalytic activity in the oxidation of thiols. *Phys. Chem. Chem. Phys.* **2007**, *9*, 3383−3396.

(10) Parra, V.; Arrieta, A. A.; Fernández-Escudero, J. A.; García, H.; Apetrei, C.; Rodríguez-Méndez, M. L.; Saja, J. A. E-tongue based on a hybrid array of voltammetric sensors based on phthalocyanines, perylene derivatives and conducting polymers: Discrimination

DOI: 10.1021/acs.jpcc.5b09707
J. Phys. Chem. C 2016, 120, 15698−15706

capability towards red wines elaborated with different varieties of grapes. *Sens. Actuators, B* **2006**, *115*, 54−61.
(11) Martín, M. G.; de Saja, J. A.; Muñoz, R.; Rodríguez-Mendez, M. L. Multisensor system based on bisphthalocyanine nanowires for the detection of antioxidants. *Electrochim. Acta* **2012**, *68*, 88−94.
(12) Volpati, D.; Alessio, P.; Zanfolim, A. A.; Storti, F. C.; Job, A. E.; Ferreira, M.; Riul, A.; Oliveira, O. N.; Constantino, C. J. L. Exploiting distinct molecular architectures of ultrathin films made with iron phthalocyanine for sensing. *J. Phys. Chem. B* **2008**, *112*, 15275−15282.
(13) Moraes, F. C.; Mascaro, L. H.; Machado, S. A. S.; Brett, C. M. A. Direct electrochemical determination of carbaryl using a multi-walled carbon nanotube/cobalt phthalocyanine modified electrode. *Talanta* **2009**, *79*, 1406−1411.
(14) Breslow, R. Biomimetic control of chemical selectivity. *Acc. Chem. Res.* **1980**, *13*, 170−177.
(15) Petty, M.; Lovett, D. R.; O'Connor, J. M.; Silver, J. Electrochromism in ytterbium bisphthalocyanine-(steric acid or cadmium stearate) films deposited by the Langmuir-Blodgett technique. *Thin Solid Films* **1989**, *179*, 387−395.
(16) Gaffo, L.; Constantino, C. J. L.; Moreira, W. C.; Aroca, R. F.; Oliveira, O. N. Atomic force microscopy and micro-Raman imaging of mixed Langmuir-Blodgett films of ytterbium bisphthalocyanine and stearic acid. *Langmuir* **2002**, *18*, 3561−3566.
(17) Gaffo, L.; Constantino, C. J. L.; Moreira, W. C.; Aroca, R. F.; Oliveira, O. N. Surface-enhanced Raman scattering and micro-Raman imaging of Langmuir−Blodgett films of rhodium phthalocyanine. *Spectrochim. Acta, Part A* **2004**, *60*, 321−327.
(18) Zucolotto, V.; Ferreira, M.; Cordeiro, M. R.; Constantino, C. J. L.; Moreira, W. C.; Oliveira, O. N. Nanoscale processing of polyaniline and phthalocyanines for sensing applications. *Sens. Actuators, B* **2006**, *113*, 809−815.
(19) Aroca, R. F.; Thedchanamoorthy, A. Vibrational studies of molecular organization in evaporated phthalocyanine thin solid films. *Chem. Mater.* **1995**, *7*, 69−74.
(20) Gaffo, L.; Constantino, C. J. L.; Moreira, W. C.; Aroca, R. F.; Oliveira, O. N. Vibrational spectra and surface-enhanced resonance Raman scattering of palladium phthalocyanine evaporated films. *J. Raman Spectrosc.* **2002**, *33*, 833−837.
(21) Treacher, K. E.; Clarkson, G. J.; Ali-Adib, Z.; McKeown, N. B. Solvent cast films derived from amphiphilic phthalocyanines: an alternative to the Langmuir-Blodgett technique for the preparation of ordered multilayer films. *Chem. Commun.* **1996**, 73−75.
(22) Griveau, S.; Gulppi, M.; Pavez, J.; Zagal, J. H.; Bedioui, F. Cobalt phthalocyanine-based molecular materials for the electrocatalysis and electroanalysis of 2-mercaptoethanol, 2-mercaptoethanesulfonic acid, reduced glutathione and L-cysteine. *Electroanalysis* **2003**, *15*, 779−785.
(23) Apetrei, C.; Rodríguez-Méndez, M. L.; Parra, V.; Gutierrez, F.; de Saja, J. A. Array of voltammetric sensors for the discrimination of bitter solutions. *Sens. Actuators, B* **2004**, *103*, 145−152.
(24) Metz, J.; Schneider, O.; Hanack, M. Synthesis and properties of substituted (phtha1ocyaninato)iron and -cobalt compounds and their pyridine adducts. *Inorg. Chem.* **1984**, *23*, 1065−1071.
(25) Stymne, B.; Sauvage, F.; Wettermark, G. A spectroscopic study of complexation of phthalocyanines with pyridine. *Spectrochim. Acta, Part A* **1980**, *36*, 397−402.
(26) Alessio, P.; Rodríguez-Méndez, M. L.; De Saja Saez, J. A. S.; Constantino, C. J. L. Iron phthalocyanine in non-aqueous medium forming layer-by-layer films: growth mechanism, molecular architecture and applications. *Phys. Chem. Chem. Phys.* **2010**, *12*, 3972−3983.
(27) Adebayo Akinbulu, I.; Nyokong, T. Fabrication and characterization of single walled carbon nanotubes-iron phthalocyanine nanocomposite: surface properties and electron transport dynamics of its self assembled monolayer film. *New J. Chem.* **2010**, *34*, 2875−2886.
(28) Adebayo, I. A.; Nyokong, T. Synthesis, spectroscopic and electrochemical properties of manganese, nickel and iron octakis-(2-diethylaminoethanethiol)-phthalocyanine. *Polyhedron* **2009**, *28*, 2831−2838.
(29) Agboola, B.; Ozoemena, K. I.; Nyokong, T. Synthesis and electrochemical characterisation of benzylmercapto and dodecylmercapto tetra substituted cobalt, iron, and zinc phthalocyanines complexes. *Electrochim. Acta* **2006**, *51*, 4379−4387.
(30) Obirai, J.; Rodrigues, N. P.; Bedioui, F.; Nyokong, T. Synthesis, spectral and electrochemical properties of a new family of pyrrole substituted cobalt, iron, manganese, nickel and zinc phthalocyanine complexes. *J. Porphyrins Phthalocyanines* **2003**, *7*, 508−520.
(31) Lever, A. B. P.; Wilshire, J. P. Electrochemistry of iron phthalocyanine complexes in nonaqueous solvents and the identification of five-coordinate iron(I) phthalocyanine derivatives. *Inorg. Chem.* **1978**, *17*, 1145−1151.
(32) Armijo, F.; Goya, M. C.; Reina, M.; Canales, M. J.; Arévalo, M. C.; Aguirre, M. J. Electrocatalytic oxidation of nitrite to nitrate mediated by Fe(III) poly-3-aminophenyl porphyrin grown on five different electrode surfaces. *J. Mol. Catal. A: Chem.* **2007**, *268*, 148−154.
(33) Arici, M.; Arican, D.; Ugur, A. L.; Erdogmus, A.; Koca, A. Electrochemical and spectroelectrochemical characterization of newly synthesized manganese, cobalt, iron and copper phthalocyanines. *Electrochim. Acta* **2013**, *87*, 554−566.
(34) Shao, J.; Richards, K.; Rawlins, D.; Han, B.; Hansen, C. A. Synthesis, electrochemistry, spectroelectrochemistry and catalytic properties in DDT reductive dechlorinationin of iron(II) phthalocyanine, 2,3- and 3,4-tetrapyridinoporphyrazine complexes. *J. Porphyrins Phthalocyanines* **2013**, *17*, 317−330.
(35) Tanaka, A. A.; Fierro, C.; Scherson, D.; Yaeger, E. B. Electrocatalytic aspects of iron phthalocyanine and its pox0 derivatives dispersed on high surface area carbon. *J. Phys. Chem.* **1987**, *91*, 3799−3807.
(36) Yu, E. H.; Cheng, S.; Logan, B. E.; Scott, K. Electrochemical reduction of oxygen with iron phthalocyanine in neutral media. *J. Appl. Electrochem.* **2009**, *39*, 705−711.
(37) Fernandes, D. M.; Ghica, M. E.; Cavaleiro, A. M. V.; Brett, C. M. A. Electrochemical impedance study of self-assembled layer-by-layer iron−silicotungstate/poly(ethylenimine) modified electrodes. *Electrochim. Acta* **2011**, *56*, 7940−7945.
(38) Wang, K.; Dai, L.; Liu, Q.; Li, H.; Ju, C.; Wu, J.; Li, H. Electrodeposition of unsubstituted iron phthalocyanine nano-structure film in a functionalized ionic liquid and its electrocatalytic and electroanalysis applications. *Analyst* **2011**, *136*, 4344−4349.
(39) Cheng, H.; Qiu, H.; Zhu, Z.; Li, M.; Shi, Z. Investigation of the electrochemical behavior of dopamine at electrodes modified with ferrocene-filled double-walled carbon nanotubes. *Electrochim. Acta* **2012**, *63*, 83−88.
(40) Lee, H.; Dellatore, S. M.; Miller, W. M.; Messersmith, P. B. Mussel-inspired surface chemistry for multifunctional coatings. *Science* **2007**, *318*, 426−430.
(41) Tran, N. L.; Kummel, A. C. A density functional theory study on the binding of NO onto FePc films. *J. Chem. Phys.* **2007**, *127*, 214701.
(42) Simic-Glavaski, B.; Zecevic, S.; Yeager, E. spectroscopic and electrochemical studies of transition-metal tetrasulfonated phthalocyanines. 3. Raman scattering from electrochemically adsorbed tetrasulfonated phthalocyanines on silver electrodes. *J. Am. Chem. Soc.* **1985**, *107*, 5625−5635.
(43) Spiro, T. G.; Strekas, T. C. Resonance Raman spectra of heme proteins. Effects of oxidation and spin state. *J. Am. Chem. Soc.* **1974**, *96*, 338−345.

DOI: 10.1021/acs.jpcc.5b09707
J. Phys. Chem. C 2016, 120, 15698−15706